Shape Optimization of a Hybrid Magnetic Torque Converter Using the Multiple Linear Regression Analysis

Sung-Jin Kim[1], Chan-Ho Kim[1], Sang-Yong Jung[2], and Yong-Jae Kim[1]

[1]Department of Electrical Engineering, Chosun University, Gwangju 61452, Korea
[2]School of Information and Communication Engineering, Sungkyunkwan University, Suwon 16419, Korea

This paper derives an effective rotor shape by the optimal design of hybrid magnetic torque converter using the multiple linear regression analysis (MLRA). In particular, using a non-linear finite-element method based on the 2-D numerical analysis, we conduct a correlation analysis between independent variables (selected by the Box–Behnken design) and reaction variable. In addition, we derive a regression equation for reaction variables according to the independent variables using the MLRA and analysis of variance. We assess the validity of the optimized design by comparing the characteristics of the optimized model derived from the response surface methodology and the initial model.

***Index Terms*— Analysis of variance (ANOVA), Box–Behnken design (BBD), hybrid magnetic torque converter (MTC), multiple linear regression analysis (MLRA), response surface methodology (RSM).**

I. Introduction

THE MAGNETIC torque converter (MTC) is a non-contact machine for torque transmission, acceleration, and deceleration. MTCs have advantages, such as no mechanical loss and maintenance-free operation. Furthermore, MTCs have inherent protection characteristics [1]–[4]. Although these MTCs have above advantages, the control of the transmission torque is impossible. This is because two rotors have permanent magnet (PM). To solve this problem, we proposed a hybrid MTC with the coils in the stator instead of the PM. This hybrid MTC with the stator structure has higher torque ripple than the conventional MTC. Therefore, the optimal design on the shape of the stator must be necessary. In this paper, the shape design is based on a Box–Behnken design (BBD). Using a non-linear finite-element method (FEM) based on the 2-D numerical analysis, an analysis is conducted between independent variables (selected by the BBD) and reaction variables. In addition, a regression equation of the reaction variable according to the independent variable, using multiple linear regression analysis (MLRA) and analysis of variance (ANOVA), is derived. The validity of the optimized design is assessed by comparing the characteristics of an optimized model derived from response surface methodology (RSM) with those of an initial model.

II. Structure of the Hybrid MTC

Fig. 1 shows the cross section of the conventional and the hybrid MTCs. The stationary pole pieces are sandwiched between high- and low-speed rotors. The 12-slot stator has one-phase concentrated windings, with the diameter of the coil and the number of turns per coil being 1.8 mm and 20, respectively. The low-speed rotor consists of a yoke made of silicon steel and 30 segment-type PMs of Br = 1.23 T. The pole piece consists of 21 steels formed by 35PN230 laminated silicon steel sheets. In addition, the gear ratio is 2.5 by the number of poles of high- and low-speed rotors [1].

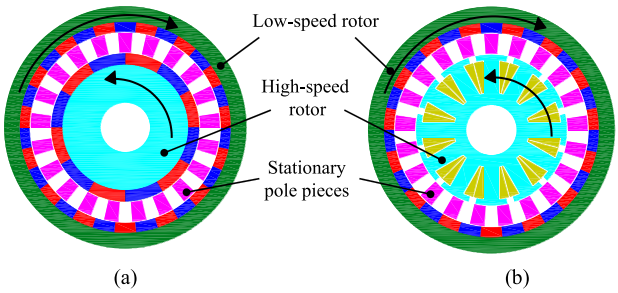

Fig. 1. Cross section of the MTC. (a) Conventional MTC. (b) Hybrid MTC.

III. Multiple Linear Regression Analysis for Shape Optimization of the Hybrid MTC

A. Response Surface Methodology

The optimal condition of the RSM is determined by the ANOVA or the DOE. Then, an analysis is conducted of the interaction formula for input variables $x_1, \ldots, x_n$ and output value y. In other words, the RSM is used to find the optimal response condition based on several factors. If there is a radius of curvature among the response variables, a response surface design is used to identify the relationship between two or more factors. When an unknown function between the design variables $x_1, \ldots, x_n$ and the dependent variable y is expressed as $f(x)$, this unknown function is called a response function. When the number of design variables x is k and the response function y is assumed to be secondary regression model, y can be expressed as

$$y = E_0 + \sum_{i=1}^{k} E_i x_i + \sum_{i=1}^{k} E_{ii} x_{ii}^2 + \sum_{i \le j}^{k} E_{ij} x_i x_j + \varepsilon \quad (1)$$

where ε represents a statistical error, which is generally assumed to be the normal distribution with a mean of

Manuscript received July 6, 2015; revised August 10, 2015; accepted September 21, 2015. Date of publication September 28, 2015; date of current version February 17, 2016. Corresponding author: Y.-J. Kim (e-mail: kimyj21@chosun.ac.kr).

Color versions of one or more of the figures in this paper are available online at http://ieeexplore.ieee.org.

Digital Object Identifier 10.1109/TMAG.2015.2482964

TABLE I
HIGH AND LOW LEVEL OF THE HIGH-SPEED ROTOR

Level		Design variable		
		α (mm)	β (mm)	γ (deg)
Low	-1	1	6	10
Central	0	2.5	7	11
High	+1	4	8	12

zero and variance of σ^2. Therefore, the response function estimated from the approximation function is expressed in vector form as

$$y = XE + \varepsilon \tag{2}$$

where X is the matrix of the design variables, E is the regression coefficient vector, and ε is the random error vector. In addition, the regression coefficient vector is estimated using the least-squares method that takes the square sum of random errors as the minimum. The least-square estimator of the regression coefficient vector is

$$E = (X'X)^{-1}X'y. \tag{3}$$

B. Box–Behnken Design

The BBD is used to efficiently estimate the first and second terms of the response-surface-estimate equation, when it is certain that all factors are not low level or high level at the same time, or when it is certain that all experiments are conducted in a stable region. The number of experiments that use the BBD is relatively smaller than that of the Central Composite Design (CCD). The BBD is useful when experiment costs are considerably expensive or practically impossible to conduct experiments at the factorial point.

On the other hand, the CCD allows for an experiment that uses a factorial point and an axial point, while the BBD allows for an experiment using the center point of the factorial point. When the CCD is used, a design at the axial point is needed. For a design at the axial point, when there are three design variables, a has a value of ± 1.682, which has an experiment point 1.682 times larger than the maximum value of the preset design variable and 1.682 times smaller than the minimum value [5]. In this case, the range of the preset design variable becomes larger and the shape of the high-speed rotor may not be formed, or design variables that cannot be designed are generated. This results in difficulties in determining the range of the initial design variables. Thus, the optimal design of the hybrid MTC was performed using the BBD. The design variables for reduction of the torque ripple of the hybrid MTC are shown in Table I and Fig. 2. An overall flowchart of the optimal design is shown in Fig. 3.

C. Multiple Linear Regression Analysis

MLRA includes the second- or third-order term for dependent variables, and interaction term between dependent variables. In Tables II–IV, degree of freedom (DF) represents the number of points that can be freely changed under the given conditions, SSR is the sum of square for regression, SSE is the sum of square for residuals, and MS is the mean square. F-value represents the test statistic for f-verification, which is used to verify whether the regression equation is significant in explaining the property of data. Where y is a result of the experiment, $\bar{y}$ is average of the y values and $\hat{y}$ is the predicted value by the regression equation. In addition, p-value is the probability of significance. When the p-value derived from this test is <0.05, the corresponding factor is considered to be significant. However, if the p-value is >0.05, the corresponding factor is not significant. Accordingly, this factor is not considered to be one that affects the dependent variables. Therefore, when performing an ANOVA, it is necessary to remove the factors of which p-value are >0.05 (i.e., the factors that are not significant) sequentially from larger values [6]. Through this process, factors of the terms of interaction and

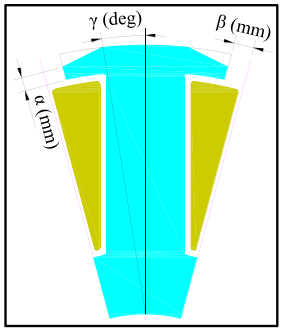

Fig. 2. Design variables of high-speed rotor.

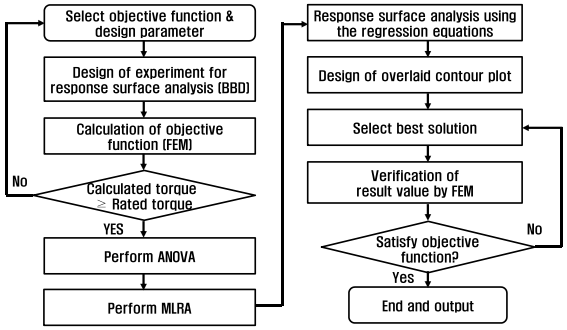

Fig. 3. Flowchart of optimal design.

TABLE II
ANOVA RESULTS OF THE HIGH-SPEED ROTOR TORQUE RIPPLE

Source	DF	SS[1)]	MS[2)]	F[3)]	P[4)]
Regression	5	131.288	26.257	7.99	0.004
Linear	3	45.368	15.122	4.60	0.032
α	1	36.019	36.018	10.96	0.009
β	1	4.536	4.536	1.38	0.270
γ	1	4.813	4.812	1.46	0.257
Square	1	68.288	68.288	20.77	0.001
$\beta\beta$	1	68.288	68.288	20.77	0.001
Interaction	1	17.632	17.631	5.36	0.046
$\beta\gamma$	1	17.632	17.631	5.36	0.046
Residual error	11	29.585	3.2872		
Total	14	160.872			

TABLE III
ANOVA RESULTS OF THE LOW-SPEED ROTOR TORQUE RIPPLE

Source	DF	SS[1)]	MS[2)]	F[3)]	P[4)]
Regression	5	0.1249	0.0249	3.38	0.054
Linear	3	0.0238	0.0079	1.08	0.407
α	1	0.0147	0.0147	2.00	0.191
β	1	0.0001	0.0007	0.03	0.876
γ	1	0.0089	0.0089	1.21	0.301
Square	1	0.0636	0.0636	8.61	0.017
$\alpha\alpha$	1	0.0636	0.0636	8.61	0.017
Interaction	1	0.0374	0.0374	5.07	0.051
$\beta\gamma$	1	0.0374	0.0374	5.07	0.051
Residual error	9	0.0665	0.0073		
Total	14	0.1915			

TABLE IV
ANOVA RESULTS OF THE LOW-SPEED ROTOR OUTPUT POWER

Source	DF	SS[1)]	MS[2)]	F[3)]	P[4)]
Regression	8	2557380	319672	189.89	0.000
Linear	3	2239197	746399	443.36	0.000
α	1	1364552	1364552	810.54	0.000
β	1	841105	841105	499.62	0.000
γ	1	33541	33541	19.92	0.004
Square	3	100957	33652	19.99	0.002
$\alpha\alpha$	1	84747	84747	50.34	0.000
$\beta\beta$	1	16084	16084	9.55	0.021
$\gamma\gamma$	1	10372	10372	6.16	0.048
Interaction	2	217226	108613	64.52	0.000
$\alpha\beta$	1	201601	201601	119.75	0.000
$\alpha\gamma$	1	15625	15625	9.28	0.023
Residual error	6	10101	1684		
Total	14	2567481			

1) $SS_{Regression} = \sum(y-\bar{y})^2$, $SS_{Error} = \sum(y-\bar{y})^2$

2) $MS_{Regression} = SS_{Regression} / k$, $MS_{Error} = SS_{Error} / n-k-1$

3) $F = MS_{Regression} / MS_{Error}$ 4) $P-value < 0.05$

factors of the terms of squares whose p-values are >0.05 were removed. Analysis was performed according to the BBD, and the results were used to perform a regression analysis of design variables α, β, and γ of the high-speed rotor. As a result of the variance analysis of the high-speed rotor torque ripple, $\alpha\alpha$ and $\gamma\gamma$ of the square term and $\alpha\gamma$ and $\alpha\beta$ of the interaction term were found to be insignificant and were removed. For the low-speed rotor torque ripple, $\beta\beta$ and $\gamma\gamma$ of the square term and $\alpha\gamma$ and $\alpha\beta$ of the interaction term were found to be insignificant and were removed. In addition, for the low-speed rotor output power, $\beta\gamma$ of the interaction term was found to be insignificant and was removed. The ANOVA results of the high- and low-speed rotor torque ripple are shown in Tables II and III, respectively. The ANOVA results of the low-speed rotor output power are shown in Table IV. In Tables II and III, the linear terms have a p-value of 0.05 or greater and, thus, they are not significant. However, because the linear term itself is significant, it is acceptable to perform the regression analysis without removing these terms.

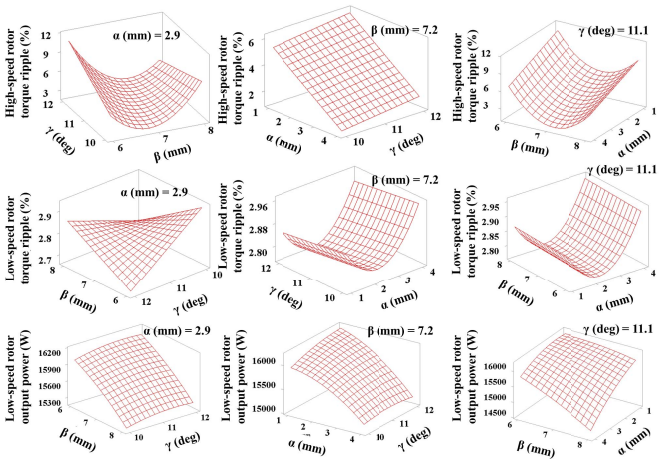

Fig. 4. Response surface of high-speed rotor torque ripple, low-speed rotor torque ripple, and low-speed rotor output power.

Thus, all the reaction variables can be estimated with a secondary model. Regression analysis equations for each design variable are

$$f_{\mathrm{HTR}}(\alpha,\beta,\gamma) = 51.7 - 1.415\alpha - 37.5\beta + 15.47\gamma + 4.277\beta\beta - 2.099\beta\gamma \quad (4)$$

$$f_{\mathrm{LTR}}(\alpha,\beta,\gamma) = 10.92 - 0.261\alpha - 1.069\beta - 0.711\gamma + 0.058\alpha\alpha + 0.0968\beta\gamma \quad (5)$$

$$f_{\mathrm{LOP}}(\alpha,\beta,\gamma) = 4299 + 1567\alpha + 974\beta + 1335\gamma - 67.33\alpha\alpha - 66\beta\beta - 53\gamma\gamma - 149.7\alpha\beta - 41.7\alpha\gamma \quad (6)$$

where $f_{\mathrm{HTR}}(\alpha,\beta,\gamma)$ and $f_{\mathrm{LTR}}(\alpha,\beta,\gamma)$ are the estimation functions of the high- and low-speed rotor torque ripple, respectively. $f_{\mathrm{LOP}}(\alpha,\beta,\gamma)$ is the estimation functions of the low-speed rotor output power.

D. Design Results and Numerical Analysis

Considering the torque ripple and output power characteristics by the design optimization, the multiobjective optimization model of hybrid MTC can be defined as

$$\textbf{\textit{s.t.}} : \{15,700 - f_{\mathrm{LOP}}(\alpha,\beta,\gamma) \le 0\} \quad (7)$$

$$\textbf{\textit{min}} : \{f_{\mathrm{HTR}}(\alpha,\beta,\gamma),\ f_{\mathrm{LTR}}(\alpha,\beta,\gamma)\}. \quad (8)$$

MLRA was performed using the results of the FEM conducted according to the BBD. Through the analysis, the high- and low-speed rotor torque ripples and the low-speed rotor output power were obtained, of which response surface plots are shown in Fig. 4. As each surface plot shows the response surface two design variables at a time, the response surface should be analyzed with one factor fixed. For this, the response surface should be analyzed using numerous surface plots. Therefore, only the surface plot that has optimal design values as the fixed values is shown. The overlaid contour plot for design variables is shown in Fig. 5. In general, the overlaid contour plot has one design variable on the x-axis and the other on y-axis. If there are three or more variables, design variable should be fixed to a certain level. In the overlaid

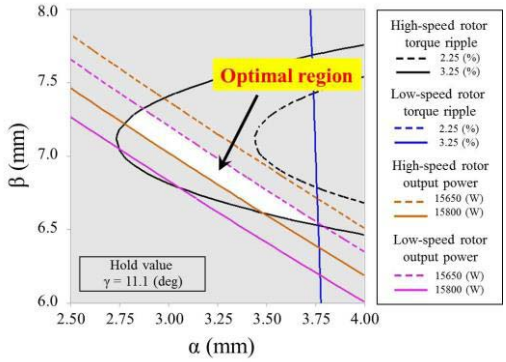

Fig. 5. Overlaid contour plot.

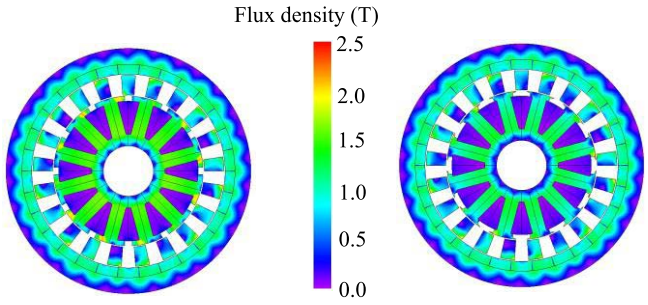

Fig. 6. Magnetic flux density contour plot. (a) Initial model. (b) Optimized model.

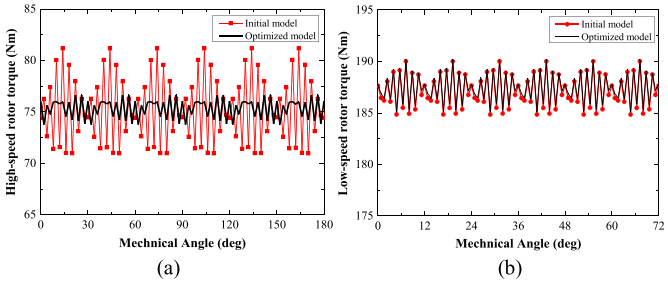

Fig. 7. Torque waveforms. (a) High-speed rotor. (b) Low-speed rotor.

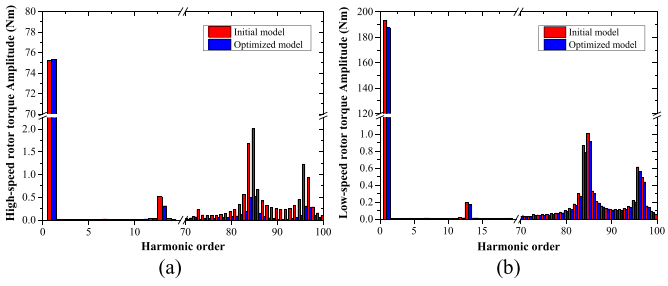

Fig. 8. Torque harmonics. (a) High-speed rotor. (b) Low-speed rotor.

contour plot, the contour plot for each response is overlaid on one graph and each contour plot represents the boundary of the response function value defined in the legend. The white region is the optimal region that satisfies all ranges indicated in the legend. Therefore, through an analysis of the response surface and the overlaid contour plot, the optimal design variable α was determined to be 2.9 mm. In addition, β was 7.2 mm and γ was 11.1°. Fig. 6 shows the magnetic flux density of the initial and optimized models. Fig. 7 shows the torque waveforms of the high- and low-speed rotors. As shown in Fig. 7, by the optimization, the high-speed rotor torque ripple was reduced by 71.8% from that of the initial model. More details about torque harmonics can be investigated with Fig. 8. As shown in Fig. 8, over the 70th harmonic components are dominant. In fact, the 85th harmonic component is the main cause for higher torque ripples in the hybrid MTC. Thus, it is mandatory to discard the specific 85th torque harmonic component as much as possible. Remarkably, it is shown that the proposed design method is very effective in compensating for the targeted 85th torque harmonic component. The optimization result is shown in Table V.

TABLE V
OPTIMIZATION RESULT

		Initial model	Optimized model
High-speed rotor	Torque (Nm)	75.23	75.32
	Torque ripple (%)	13.57	3.82
	Output power (kW)	15.7	15.7
Low-speed rotor	Torque (Nm)	187.17	187.45
	Torque ripple (%)	2.76	2.66
	Output power (kW)	15.6	15.7

IV. CONCLUSION

In this paper, an effective shape to reduce the torque ripple of the hybrid MTC is derived from a BBD. An analysis is conducted between independent variables selected by the BBD and reaction variables using the non-linear FEM based on the 2-D numerical analysis. In addition, the regression equation of the reaction variables is derived according to the independent variable by the MLRA and ANOVA. As a result, the torque ripple of the high-speed rotor was reduced by 71.8% from that of the initial model and torque ripple of the low-speed rotor was reduced by 3.6%.

ACKNOWLEDGMENT

This work was supported by research funds through Chosun University, Gwangju, Korea, in 2011.

REFERENCES

[1] K. Atallah and D. Howe, "A novel high-performance magnetic gear," *IEEE Trans. Magn.*, vol. 37, no. 4, pp. 2844–2846, Jul. 2001.
[2] P. O. Rasmussen, T. O. Andersen, F. T. Jørgensen, and O. Nielsen, "Development of a high-performance magnetic gear," *IEEE Trans. Ind. Appl.*, vol. 41, no. 3, pp. 764–770, May/Jun. 2005.
[3] N. Niguchi and K. Hirata, "Torque-speed characteristics analysis of a magnetic-geared motor using finite element method coupled with vector control," *IEEE Trans. Magn.*, vol. 49, no. 5, pp. 2401–2404, May 2013.
[4] K. T. Chau, D. Zhang, J. Z. Jiang, C. Liu, and Y. Zhang, "Design of a magnetic-geared outer-rotor permanent-magnet brushless motor for electric vehicles," *IEEE Trans. Magn.*, vol. 43, no. 6, pp. 2504–2506, Jun. 2007.
[5] B.-H. Lee, J.-P. Hong, and J.-H. Lee, "Optimum design criteria for maximum torque and efficiency of a line-start permanent-magnet motor using response surface methodology and finite element method," *IEEE Trans. Magn.*, vol. 48, no. 2, pp. 863–866, Feb. 2012.
[6] S.-J. Kim, C.-H. Kim, S.-Y. Jung, and Y.-J. Kim, "Optimal design of novel pole piece for power density improvement of magnetic gear using polynomial regression analysis," *IEEE Trans. Energy. Convers.*, vol. 30, no. 3, pp. 1171–1179, Sep. 2015.